

High-precision determination of structure factors F_h of silicon

R. Teworte and U. Bonse

Institut für Physik, Universität Dortmund, Postfach 50 05 00, D-4600 Dortmund 50, Federal Republic of Germany

(Received 4 May 1983)

Structure factors F_h of perfect silicon crystals have been measured at room temperature for a number of 16 reflections up to the (880) for both Ag $K\alpha_1$ and Mo $K\alpha_1$ radiation. The measurements are based on the analysis of the fine oscillatory structure of Laue case rocking curves. The data are consistent with earlier results obtained with the pendellösung method using wedge-shaped crystals, but probable errors were reduced to below the 0.1% level. An important advantage of the new method is the significantly reduced ideal crystal volume of typically 0.5 mm^3 for silicon and material with similar absorption, which makes it applicable even if large perfect crystals are difficult, or practically impossible, to grow.

I. INTRODUCTION

The pendellösung fringe method with wedge-shaped crystals, proposed by Kato and Lang in 1959,¹ made feasible for the first time a structure-factor determination with an accuracy better than 0.5% and, simultaneously, put the data on an absolute scale. As a consequence, structure-factor values became an additional important test of crystal-binding theories and band-structure calculations.²⁻⁸ This is mainly due to the fact that on a 0.1% precision level free-atom wave functions no longer describe the scattering amplitude adequately, since the aspherical distribution of valence electrons must be taken into account. Unfortunately, because of the high degree of crystal perfection necessary throughout a wedge of several millimeters height, very few materials have been experimented with, namely silicon,⁹⁻¹¹ germanium,¹² and quartz.¹³ The most comprehensive studies were carried out with silicon, where a number of reflections were measured by Hattori *et al.*⁹ and, with increased precision, by Aldred and Hart.¹¹ Besides the latter, only one further group stated probable errors on the 0.1% level for a few reflections,¹⁰ but discrepancies between these measurements amounted to almost 0.4%.

Apart from the pendellösung fringe method, several other methods for high-precision measurements of structure factors were elaborated, such as (a) the reflection profile method,¹⁴ (b) the evaluation of the fine structure of Bragg and Laue case reflection curves from thin single crystals,¹⁵ or (c) the pendellösung effect with a white incident beam.¹⁶ As compared to the pendellösung fringe method, all of them have less accuracy (about 0.5% at best), but they have the advantage of a considerably smaller perfect-crystal region needed as a specimen.

It is the purpose of this paper to show that with the rocking-curve method in the Laue case¹⁷ structure factor determinations can be performed with at least the high precision of the pendellösung fringe method, but with significantly (e.g., about 2 orders of magnitude) reduced perfect-crystal volume. In order to demonstrate the strength of the new method experiments were carried out

with silicon crystals, offering the possibility of direct comparison with the previous measurements mentioned above.

II. THEORY

With the use of the ray geometry shown in Fig. 1, the intensity of the twice-reflected beam R_0 as a function of the angle $\delta\theta$ between the net planes of crystals 1 and 2 is calculated both in plane-wave¹⁷ and in spherical-wave¹⁸ theory to be proportional to the convolution integral

$$R_0(\delta\theta) \approx \sum_{\alpha} \int_{-\infty}^{\infty} I_{R1}^{\alpha}(\theta) I_{R2}^{\alpha}(\theta + \delta\theta) d\theta, \quad (1)$$

where the sum is taken over the polarization states $\alpha = \sigma, \pi$ with $C^{\sigma} = 1$, $C^{\pi} = \cos 2\theta_B$. Indices 1 and 2 distinguish crystals 1 and 2. The single-crystal intensity $I_R^{\alpha}(\theta)$ for crystals with thickness t is given as

$$I_{Rj}(\theta) = \left| \sin \left[\frac{\pi t}{\Delta_e^{\alpha}} Y(\theta) \right] / Y(\theta) \right|^2, \quad (2)$$

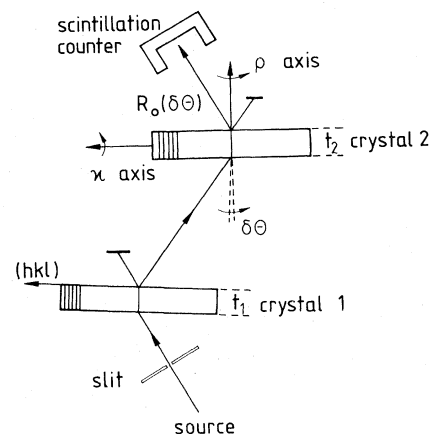


FIG. 1. Ray geometry for the symmetric Laue case. Intensity $R_0(\delta\theta)$ is measured integrally over the full width of the outgoing beam. The κ axis is normal to the Bragg planes (hkl) , the $\delta\theta$ axis is normal to the plane of the figure, and the ρ axis is normal to both the κ and $\delta\theta$ axis.

with $Y(\theta)$ measuring the deviation $\theta - \theta_B$ of the incoming beam from the kinematical Bragg angle θ_B :

$$Y(\theta) = \left\{ \frac{(\Delta_e^\alpha)^2}{d^2} \left[(\theta - \theta_B) \frac{\cos \theta_B}{\gamma_h} + \frac{\chi_0}{4 \sin \theta_B} \left[\frac{1}{\gamma_h} - \frac{1}{\gamma_0} \right] \right]^2 + \nu^2 \right\}^{1/2}. \quad (3)$$

d is the spacing of the net planes used. ν^2 is a function of the complex Fourier coefficients $\chi_h, \chi_{\bar{h}}$ of the dielectric polarizability $\chi(\vec{r})$,

$$\nu^2 = \frac{\chi_h \chi_{\bar{h}}}{|\chi_h \chi_{\bar{h}}|}, \quad (4)$$

and can, for low absorption, be approximated by¹⁷

$$\nu^2 = 1 - i \frac{\chi_{ih} \mu_0 \Delta_e^\alpha |C^\alpha|}{\chi_{i0} \pi (\gamma_0 \gamma_h)^{1/2}}. \quad (5)$$

χ_{i0}, χ_{ih} are the imaginary parts of the Fourier coefficients χ_0, χ_h ; μ_0 is the normal absorption coefficient; γ_0 and γ_h measure the angle between the crystal-surface normal \vec{z} and the directions \vec{k}_0 and \vec{k}_h of the incoming and reflected beams:

$$\gamma_0 = \frac{\vec{k}_0}{|\vec{k}_0|} \cdot \vec{z}, \quad \gamma_h = \frac{\vec{k}_h}{|\vec{k}_h|} \cdot \vec{z}. \quad (6)$$

The polarization-dependent extinction length Δ_e^α is related to the structure factor F_h according to

$$\Delta_e^\alpha = \frac{\lambda (\gamma_0 \gamma_h)^{1/2}}{|C^\alpha (\chi_h \chi_{\bar{h}})^{1/2}|} = \frac{V_c (\gamma_0 \gamma_h)^{1/2}}{\lambda |C^\alpha|} \frac{\pi}{r_e} \frac{1}{|F_h|}. \quad (7)$$

Here, V_c is the volume of the unit cell, λ is the wavelength used, and r_e is the classical electron radius. Typical values of Δ_e^α range from 30 to 200 μm for silicon crystals.

For monatomic crystals of the diamond structure within the spherical atom approximation, the structure factor F_h is connected with the atomic form factor f_h according to

$$F_h = 8a_h f_h, \quad (8)$$

where

$$a_h = \begin{cases} 1 & \text{for } h, k, l \text{ all even and } h + k + l = 4n \\ 1/\sqrt{2} & \text{for } h, k, l \text{ all odd} \\ 0, & \text{otherwise.} \end{cases} \quad (9)$$

The shape of the rocking curve depends on the extinction length Δ_e^α and therefore, apart from some geometrical factors, on the structure factor F_h in two ways: (a) Δ_e^α is part of the conversion factor equation (3) connecting absolute angle θ and the angular dependence function $Y(\theta)$, and (b) together with the crystal thickness Δ_e^α determines the periodicity and the imaginary damping part of the sin function of Eq. (2). As a consequence, both the angular scale and the precise shape of the convoluted curve R_0 are

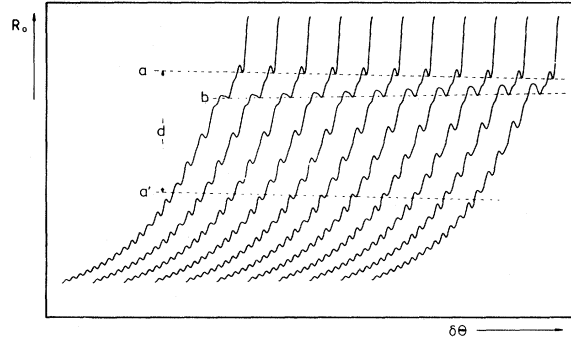


FIG. 2. Left wings of calculated rocking curves $R_0(\delta\theta)$ for silicon (800), $\text{MoK}\alpha_1$ radiation. Crystal thickness is $t_1 = 689.0 \mu\text{m}$, $t_2 = 699.1 \mu\text{m}$. Δ_e^α is diminished in steps of $0.0738 \mu\text{m}$ from $81.623 \mu\text{m}$ on the left to $80.886 \mu\text{m}$ on the right. $\Delta_e^\pi = \Delta_e^\alpha / |C^\pi|$. Line a , its parallel a' , and line b help to visualize the change in the positions of the subsidiary extrema.

$|F_h|$ dependent. In low-absorption cases ($\mu t \leq 1-2$) the imaginary part is small compared to 1, and especially the shape becomes extremely sensitive to Δ_e^α variations. This is clearly demonstrated in the series of half-rocking curves in Fig. 2 calculated with Δ_e^α diminishing in steps of $0.0738 \mu\text{m}$ from 81.623 to $80.886 \mu\text{m}$ and Δ_e^π varying correspondingly [Eq. (7)]. For a given experimental curve, it is quite straightforward to select the best fitting computed curve, thereby determining the absolute value of Δ_e^α to better than 0.1%.¹⁷ With knowledge of V_c , λ and the geometrical factor $(\gamma_0 \gamma_h)^{1/2}$, $|F_h|$ is obtained.

Of equal influence as Δ_e^α in Eq. (2) is the crystal thickness t , which therefore must be measured with corresponding precision. On the other hand, it is *not* essential that both crystals have exactly the same thickness. As can be seen in Fig. 3, changes in t of just one crystal can be clearly separated from equal thickness changes in both crystals, which is, except for the absolute θ scale, equivalent to a change of $|F_h|$ in our calculations. This fact is important with respect to precision, because thus only *one* error of thickness t is introduced in the results.

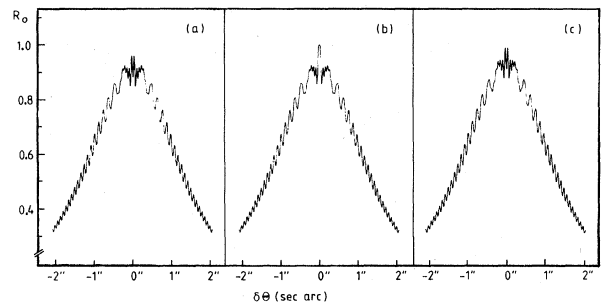


FIG. 3. Influence of crystal-thickness changes on the shape of the rocking curve R_0 . Calculations were done for silicon (220), $\text{AgK}\alpha_1$ radiation, $|f_h| = 8.436$; (a): $t_1 = 689 \mu\text{m}$, $t_2 = 699 \mu\text{m}$; (b): $t_1 = 691 \mu\text{m}$, $t_2 = 699 \mu\text{m}$; (c): $t_1 = 691 \mu\text{m}$, $t_2 = 701 \mu\text{m}$.

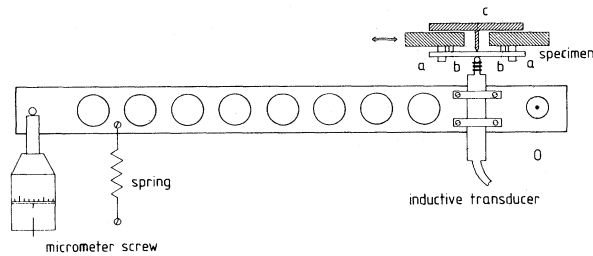


FIG. 4. Lever system to measure the crystal thickness with an accuracy of better than $0.1 \mu\text{m}$. The lever can be rotated around 0. Specimen leans against two steel tips b and is supported by polished steel pins a . It is pressed against a third tip c by the inductive transducer which is set to zero reading with the help of the micrometer screw. The system is calibrated with gauge plates of different thicknesses as specimens. With a total length of 1 m the lever reduces the micrometer movement by a factor of 20.

III. EXPERIMENTAL

The experiment was carried out using conventional sealed-off x-ray tubes. Crystal thickness t is critical on one side because of the necessity for measuring its absolute values to better than 0.1%, which is much easier for thick crystals. On the other hand, there is stringent demand to keep $\mu_0 t$ well below 2. An additional advantage of thick crystals is the increasing total number n of oscillations on the wings of the rocking curve ($n \approx t/\Delta_e$), which may be used in the fitting process.

Parallel-sided samples were prepared from a $\langle 111 \rangle$ -grown float-zone crystal with a residual strain of 2×10^{-8} (labeled no. 6 in Ref. 19). The surface normal chosen was $\langle 110 \rangle$, which allows one to measure a high number of reflections in the symmetrical Laue case with many of them being barely affected by growth striations.¹⁷ In the cutting process, any deviation from the $\langle 110 \rangle$ direction was kept below $1'$ by proper alignment of crystal and diamond saw using a low-index x-ray reflection. After a conventional etching procedure, usually a surface roughness of several micrometers remains, which makes a precise thickness determination impossible and, at the same time, smears out the fine oscillations on the wings of the rocking curve. Therefore a final mechanical-chemical etching process was used, which is known to produce a surface flatness of better than 1000 \AA , still retaining a strain-free surface.²⁰ With a contact-free optical thickness measurement system incorporating a traveling microscope with a resolution of $\pm 1 \mu\text{m}$, a pair of crystals with $t_1 = 699.5 \mu\text{m}$ and $t_2 = 691.0 \mu\text{m}$ and high plane parallelism was selected. After the experiment the crystal thickness was determined with the help of the high-precision lever system shown in Fig. 4. By comparison with calibrated thickness gauge plates, an accuracy of better than $\pm 0.1 \mu\text{m}$ was achieved. It was found that both crystal plates were slightly wedge shaped with a thickness gradient of $(0.16, 0.12) \mu\text{m mm}^{-1}$ and $(0.0, 0.7) \mu\text{m mm}^{-1}$ in $(\langle 110 \rangle, \langle 001 \rangle)$ directions for crystals 1 and 2, respectively.

As described in an earlier paper,¹⁷ the crystals were standing on two screws, leaning slightly against a third at the top. Although no glue was used, the mounting proved to be stable, even if the crystals were tilted within their surface plane by more than 30° as was necessary in the case of the (111) reflection. The beam position on the crystals was determined to $\pm 0.5 \text{ mm}$ with the help of an appropriate diaphragm which could be positioned in front of each crystal. In the beam plane (i.e., the plane which is extended by the incident and diffracted beams), the width x_e of the beam is increased due to the energy spread within the whole Borrmann fan. At the exit surface of the second crystal it is given by

$$x_e = f / \cos \theta_B + 2(t_1 + t_2) \tan \theta_B, \quad (10)$$

where f is the width of the focus or of the slit in front of the first crystal, whichever is smaller. The beam height h is purely determined by the geometrical divergence of the beam and can be kept as low as intensity demands allow. In our experiments, typically $f \approx 0.8 \text{ mm}$ and $h = 0.5 \text{ mm}$.

If the surface normal makes an angle κ with the beam plane (Fig. 1), the effective crystal thickness t' is enlarged to

$$t' = t / \cos \kappa. \quad (11)$$

During the experiments, κ was controlled to better than 0.1° to avoid any errors. A misalignment in ρ smears out the rocking curve and by means of piezoelectric transducer ρ could be adjusted to better than $1''$. The angular resolution required to measure the fine structure of the rocking curve is extremely high. The evaluation of Eq. (3) for large values of $\theta - \theta_B$ results in an angular increment $\Delta\theta \approx d/t$ in angle between subsequent maxima. In order to resolve this structure in the most extreme case of the (880) reflection of silicon, where $d/t \approx 6.9 \times 10^{-8}$ corresponding to $\Delta\theta = 0.014''$, curves were measured at intervals as small as $10^{-3}''$. An appropriate rotation table of high stability and reproducibility was described elsewhere.²¹

Rocking curves contained between 30 and 250 extrema depending on wavelength and reflection chosen. For precise determination of the extrema intensity, each curve was resolved into 500–3200 points, which were measured each with a statistical error of typically 1%. The counting system consisted of a NaI scintillation counter with pulse height discrimination in order to exclude harmonics if necessary. Total time of measurement was from 4 to 20 h for one curve. For each reflection, at least four rocking-curve scans were made. Stability was improved by an antivibration base with a resonance frequency of 1.7 Hz and a thermal shield reducing room-temperature fluctuations to far below 0.1 K.

IV. DATA EVALUATION AND RESULTS

In a first step the relative heights of the extrema of experimental rocking curves are compared to those of sets of theoretical curves similar to Fig. 2, thereby determining the value for Δ_e . Slight thickness variations in vertical direction (perpendicular to the beam plane) within the

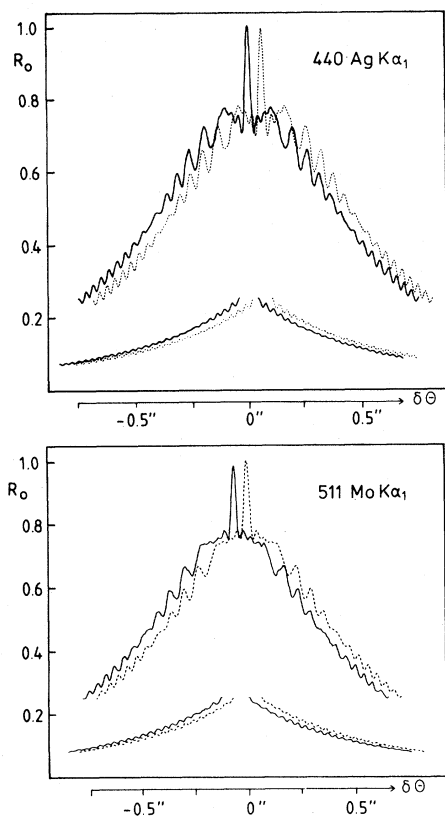


FIG. 5. Two examples of the excellent agreement between the measured solid curve and the corresponding theoretical dashed curve, shifted slightly to the right. Tails of the rocking curves have been shifted horizontally towards the center.

beam occur for crystal 2 due to the relatively large thickness gradient of $0.7 \mu\text{m mm}^{-1}$ in the $\langle 001 \rangle$ direction. In our calculations this is taken into account by averaging curves with appropriately chosen values of t_2 . For some reflections [mainly (400), (800)], crystal 2 is slightly wedge shaped in the horizontal direction as a result of the thickness gradient. In this case, as can be shown by numerical calculation of beam paths in the spherical-wave case,²² the rocking curves become slightly asymmetrical (about 1% difference in height of corresponding extrema on both wings), but the left-right averaged value remains unchanged and no additional error has to be taken into consideration. Two examples of the excellent correspondence between experimental and theoretical curves are shown in Fig. 5.

In our calculations the parameters occurring in the imaginary part of ν^2 [Eq. (5)] have values

$$\mu_0 = \begin{cases} 0.732(\text{Ag } K\alpha_1) \\ 1.46(\text{Mo } K\alpha_1) \end{cases}$$

measured in mm^{-1} , taken from Ref. 23,

$$\frac{\chi_{ih}}{\chi_{i0}} = a_h D_h (1 - E^\alpha 2Q \sin^2 \theta_B),$$

with

$$E^\alpha = \begin{cases} 1 & \text{for } \alpha = \sigma \\ 1 + \frac{2 \cos^2 \theta_B}{\cos 2\theta_B} & \text{for } \alpha = \pi \end{cases}$$

and

$$Q = \begin{cases} 0.0591 & (\text{Ag } K\alpha_1) \\ 0.0463 & (\text{Mo } K\alpha_1) \end{cases}$$

from Ref. 24, where a_h is given by Eq. (9).

For the calculation of the Debye-Waller factor D_h , a Debye temperature of $\Theta_D = 543 \text{ K}$ (Refs. 9 and 25) was assumed. This value was used also for the reduction of the structure factors to a common temperature of 20°C .¹⁰ It should be noted that calculations are not very sensitive to the precise value of the imaginary part of ν^2 , e.g., to the stated values of μ_0 and χ_{ih}/χ_{i0} , so variations of its value of 5% do not change the resultant data for Δ_e .

From Δ_e we calculate structure factors F_h and, together with Eq. (8), atomic form factors f_h using

$$\lambda = \begin{cases} 0.5594227(7) & (\text{Ag } K\alpha_1) \\ 0.7093185(4) & (\text{Mo } K\alpha_1) \end{cases}$$

(measured in \AA) from Ref. 26 and

$$V_c = a_0^3$$

with

$$a_0 = 5.43102018(34)$$

in \AA at 22.5°C , taken from Ref. 27.

No additional error is introduced in this final calculation because of the high precision of these parameters. Furthermore, there is no need to pay attention to the thermal expansion coefficient for silicon [$\alpha \approx 2.6 \times 10^{-6} \text{ K}^{-1}$ (Ref. 28)]. We would also like to point out that because of the natural width of the $K\alpha_1$ line, oscillations are slightly smeared out. This effect can be calculated easily and does not additionally alter the shape of the curves.

A major point which has not been discussed so far is the influence of the minute residual strain present in our specimen, consisting of both local lattice rotations and $\Delta d/d$ fluctuations of 2×10^{-8} as mentioned above. Mainly reflections from net planes (hkl), not including an angle of 90° to the growth axis, might be influenced. This effect was carefully considered by numerical computation of resulting curved beam paths and the changed phase integrals applying the ray optical theory in the form given by Bonse²⁹ to our problem of a spherical wave incident on a double-crystal Laue geometry. As a result calculations give asymmetric rocking curves with smeared-out oscillations only for strain coefficients significantly higher than those we have to consider.^{22,30}

Table I lists our results together with results from earlier measurements. The probable errors given in parentheses are mainly determined from the fitting process of measured and calculated curves. A second contribution, amounting to 2.8×10^{-4} , is given by the uncertainty in the crystal thicknesses and the beam position.

TABLE I. Present results of atomic scattering factors f_h of silicon for $T=293.2$ K and comparison with earlier measurements. Probable errors are given in parentheses except for AH's values where the mean derivation is given.

Reflection	Present work		AH ^a		Others
	Ag $K\alpha_1$	Mo $K\alpha_1$	Ag $K\alpha_1$	Mo $K\alpha_1$	Ag $K\alpha_1$
(111)	10.658(5)	10.699(6)	10.668(6)	10.706(5)	10.664(2) ^b
(220)	8.440(5)	8.487(10)	8.439(8)	8.483(6)	8.463(1) ^b
(311)	7.738(5)	7.771(6)	7.746(9)	7.773(7)	
(400)	7.053(4)	7.074(4)	7.054(8)	7.079(10)	
(331)	6.787(4)	6.803(4)	6.786(8)	6.815(7)	
(422)	6.158(4)	6.200(4)	6.163(9)	6.210(9)	
(333)	5.835(5)	5.863(3)	5.832(5)	5.869(7)	5.843(2) ^b
(511)	5.844(5)	5.878(4)	5.846(5)	5.877(7)	
(440)	5.389(4)	5.413(4)	5.390(8)	5.414(4)	5.408(2) ^b
(444)	4.170(3)	4.205(6)	4.178(4)	4.202(5)	4.172 ^b
(551)	3.983(4)	4.008(3)			4.100(20) ^c
(800)	3.288(4)	3.322(3)			
(660)	2.960(2)	2.988(2)	2.966(9)	2.988(7)	
(555)	2.848(4)	2.870(4)	2.843(3)	2.865(7)	
(844)	2.198(3)	2.227(4)	2.194(8)	2.211(6)	
(880)	1.575(4)		1.578(4)	1.589(8)	

^aReference 11, corrected for the more precise value of $a_0=5.431$ Å.

^bReference 10, without correction for nuclear scattering.

^cReference 9.

V. CONSISTENCY OF THE MEASUREMENTS

On the 0.1% level there are only two more data sets available for comparison. For the (111), (333), and (444) reflections, all three measurements agree to within 0.2%, whereas in the case of the (220) and (440) reflections, our results agree with those obtained by Aldred and Hart (AH) (maximum deviation 0.04%), but are certainly not consistent with those of Tanemura and Kato. This supports the argumentation of AH, who pointed out that the crystals of Tanemura and Kato were likely to be influenced by inhomogeneous strain for these reflections. For the other reflections—except (551) and (800), where no other precise value is known—only AH's data are available. Up to the (444), only 3 out of 20 values deviate by more than 0.1%, thus demonstrating excellent agreement and strongly indicating the high reproducibility of structure-factor data obtained with quite independent methods. All other results except for the Mo (844) value agree to within 0.2%. There is slight indication (see Fig. 6) that AH's (844) value might be too low.

A rather straightforward test for internal consistency is a logarithmic plot of the differences in structure factors for Mo and Ag radiation versus $\sin^2\theta/\lambda^2$.¹¹ This has been done for both ours and AH's measurements in Fig. 6. Assuming a dispersion correction which is independent of $\sin\theta/\lambda$ except for the Debye-Waller factor $D_h = \exp(-B \sin^2\theta/\lambda^2)$, we expect a straight line of slope $-B$ giving the value for $\Delta f' = f_{\text{Mo}} - f_{\text{Ag}}$ in forward direction as the intercept with the ordinate. While our measurements give $\Delta f' = (36 \pm 4) \times 10^{-3}$ and $B = 0.40 \pm 0.24$, where B is in good agreement with the expected value of 0.444, AH's data result in $\Delta f' = (40 \pm 3) \times 10^{-3}$ and $B = 1.00 \pm 0.23$, indicating that the differences in the form factors are too low for higher hkl values. On the other

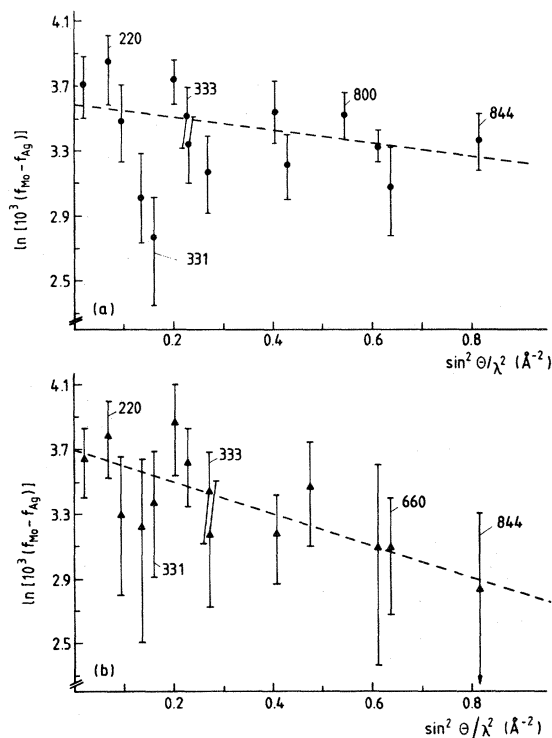


FIG. 6. (a) Internal consistency test between the results obtained for Ag $K\alpha_1$ and Mo $K\alpha_1$ wavelengths, see text. Error bars indicate probable errors. Dashed line is a least-square fit excluding the (331) data. (b) Same as (a), but using AH's data set (Ref. 11). Note the longer error bars in (b).

hand, there is some indication, especially regarding the seven low-order reflections, that the variation of $\Delta f'$ with $\sin\theta/\lambda$ might be more complicated than assumed in this simple model.

In Table II Δf values are listed resulting from both experiment and theory. Our value of 36×10^{-3} is higher than theoretical estimates and Cusatis's interferometric measurement, but it is in better agreement with them than is AH's value. With respect to the data of Takeda and Kato, it should be noted that their value is measured with pendellösung fringes using a total of five wedge-shaped crystals. However, there is doubt that their value is reliable, because different specimens gave a wide distribution between 16.9×10^{-3} and 39.8×10^{-3} for $\Delta f'$.

VI. CONCLUSIONS

We have shown that absolute structure measurements down to the 0.05% level can be performed with the rocking-curve method in the Laue case. The accuracy which can be achieved depends essentially on how much the shape of the computed rocking curves changes with varying $|F_h|$ values. The results obtained for silicon agree well with former measurements made with the pendellösung fringe method. In comparison errors of the present method are lower by 50%. Two major advantages of the new method make it applicable to less favorable cases when only small perfect crystals are available:

(i) The perfect-crystal volume of the specimen is limited solely by the existence of the Borrmann fan [see Eq. (10)] and is typically 2 orders of magnitude smaller compared

TABLE II. Comparison of experimental and theoretical values for differences in atomic form factors for $\text{MoK}\alpha_1$ and $\text{AgK}\alpha_1$ wavelengths.

	$(f_{\text{Mo}} - f_{\text{Ag}}) \times 10^3$
Present work	36 ± 4
Aldred ^a	39 ($T=293.2$ K)
	29 ($T=92.2$ K)
Price, Maslen, and Mair ^b	38
Cusatis and Hart ^c	29 ± 3
Takeda and Kato ^d	25.5 ± 2.4
Gerward <i>et al.</i> ^e	29
Cromer and Liberman ^f	30
Wagenfeld ^g	30 theoretical

^aReference 31.

^bReference 32.

^cReference 33.

^dReference 34.

^eReference 35.

^fReference 36.

^gReference 37.

to the pendellösung fringe method. A total volume below 0.5 mm^3 is easily achievable.

(ii) Lattice strain influences are readily detected by asymmetry in the rocking curve and/or smearing out of the oscillations, so that it is easy to choose a crystal region of sufficient perfection while aligning the double-crystal geometry.

¹N. Kato and A. R. Lang, *Acta Crystallogr.* **12**, 787 (1959).

²P. F. Price, E. N. Maslen, and S. L. Mair, *Acta Crystallogr. A* **34**, 183 (1978).

³M. Fehlmann, *J. Phys. Soc. Jpn.* **47**, 225 (1979).

⁴U. Pietsch, *Phys. Status Solidi B* **102**, 127 (1980).

⁵U. Pietsch and K. Unger, *Phys. Status Solidi B* **102**, 503 (1980).

⁶C. Scheringer, *Acta Crystallogr. A* **36**, 205 (1980).

⁷C. S. Wang and B. M. Klein, *Phys. Rev. B* **24**, 3393 (1981).

⁸M. T. Yin and M. L. Cohen, *Phys. Rev. B* **26**, 5668 (1982).

⁹H. Hattori, H. Kuriyama, T. Katagawa, and N. Kato, *J. Phys. Soc. Jpn.* **20**, 988 (1965).

¹⁰S. Tanemura and N. Kato, *Acta Crystallogr. A* **28**, 69 (1972).

¹¹P. J. E. Aldred and M. Hart, *Proc. R. Soc. London Ser. A* **332**, 223 (1973).

¹²B. W. Batterman and J. R. Patel, *J. Appl. Phys.* **39**, 1882 (1968).

¹³K. Yamamoto, S. Homma, and N. Kato, *Acta Crystallogr. A* **24**, 232 (1968).

¹⁴S. Kikuta, T. Matsushita, and K. Kohra, *Phys. Lett.* **33A**, 151 (1970).

¹⁵M. Renninger, *Acta Crystallogr. A* **31**, 42 (1975).

¹⁶T. Takama, M. Iswasaki, and S. Sato, *Acta Crystallogr. A* **36**, 1025 (1980).

¹⁷U. Bonse and R. Teworte, *J. Appl. Crystallogr.* **13**, 410 (1980).

¹⁸U. Bonse and R. Teworte, *Z. Naturforsch.* **37A**, 427 (1982).

¹⁹U. Bonse and I. Hartmann, *Z. Kristallogr.* **156**, 265 (1981).

²⁰L. H. Blake and E. Mendel, IBM TR 19.0062 (1969).

²¹U. Bonse and R. Teworte, *J. Phys. E* **15**, 187 (1982).

²²R. Teworte, Thesis, University of Dortmund, 1982 (unpublished).

²³Experimental values given by G. Hildebrandt, J. D. Stephenson, and H. Wagenfeld, *Z. Naturforsch.* **28A**, 588 (1973).

²⁴Theoretical values given by G. Hildebrandt, J. D. Stephenson, and H. Wagenfeld, *Z. Naturforsch.* **30A**, 696 (1975).

²⁵B. W. Batterman and D. R. Chipman, *Phys. Rev.* **127**, 690 (1962).

²⁶E. G. Kessler, Jr., R. D. Deslattes, D. Girard, W. Schwitz, L. Jacobs, and O. Renner, *Phys. Rev. A* **26**, 2696 (1982).

²⁷P. Becker, P. Seyfried, and H. Siegert, *Z. Phys. B* **48**, 17 (1982).

²⁸K. G. Lyon, G. L. Salinger, C. A. Swenson, and G. K. White, *J. Appl. Phys.* **48**, 865 (1977).

²⁹U. Bonse, *Z. Phys.* **177**, 385 (1964).

³⁰R. Teworte and U. Bonse (unpublished).

³¹P. J. E. Aldred, Thesis, University of Bristol, 1971 (unpublished).

³²Analysis of AH's data set with refined pseudoatom density functions is given by P. F. Price, E. N. Maslen, and S. L. Mair, *Acta Crystallogr. A* **34**, 183 (1978).

³³C. Cusatis and M. Hart, in *Anomalous Scattering*, edited by S. Ramaseshan and S. C. Abrahams (Munksgaard, Copenhagen, 1975), p. 57.

³⁴T. Takeda and N. Kato, *Acta Crystallogr. A* 34, 43 (1978).

³⁵This value was obtained by a Kramers-Kronig transformation of absorption measurements by L. Gerward, G. Thuesen, M. Stibius Jensen, and I. Alstrup, *Acta Crystallogr. A* 35, 852 (1979).

³⁶D. T. Cromer and D. Liberman, *J. Chem. Phys.* 53, 1891 (1970).

³⁷H. Wagenfeld, in *Anomalous Scattering*, edited by S. Ramaseshan and S. C. Abrahams (Munksgaard, Copenhagen, 1975), p.13.